*Anal. Bioanal. Electrochem., Vol. 11, No. 10, 2019, 1383-1397*

***Analytical & Bioanalytical Electrochemistry***

2019 by CEE
www.abechem.com

*Full Paper*

# Electrochemical Investigation of Uric Acid using MWCNTs-Decorated Novel Substituted Cobalt(II) Phthalocyanine Modified GCE

**Malathesh Pari and Kallam Ramareddy Venugopala Reddy***

*Department of Chemistry, Vijayanagara Sri Krishnadevaraya Univarsity, Ballari,-583105 Karnataka, India*

*Corresponding Author, Tel.: +9448170456

E-Mail: Venugopalareddy@vskub.ac.in

*Received: 24 July 2019 / Received in revised form: 17 October 2019 / Accepted: 19 October 2019 / Published online: 31 October 2019*

**Abstract**- The present work is very simple and sensitive method for cyclic voltammetry, differential pulse voltammetry and chrono amperometry (CA). Uric acid sensor was developed at (DBCMAT-CoPcs) 2,4-dibromo-6-{[cyclohexyl(methyl)amino]methyl}aniline-tetra substituted on cobalt phthalocyanine modified GCE. The novel synthesized catalyst confirmed with various spectroscopic techniques. The modified DBCMAT-CoPc/GCE showed a high electrocatalytic activity and lower potential towards the oxidation of uric acid (UA). The response of UA was linear over the concentration ranging from (CV 0.1–1.8; DPV 0.2–2.8; CA 0.05–0.8 µmol/L), sensitivity for (CV 131.85; DPV 22.634; CA 2.509 $\mu A \mu M^{-1} cm^{-2}$) and detection limit for (CV 0.03; DPV 0.066; CA 0.016 µM) (S/N=3). The CVs and DPV techniques shows the same peak potential (+370 mV) and fabricated sensor exhibited its special advantages such as low working potential, sensitivity along with good repeatability and reproducibility for the determination of uric acid.

**Keywords-** Cobalt phthalocyanine, Cyclic voltammetry, Differential pulse voltammetry, Amperometry, Uric acid, Chemically modified electrode

## 1. INTRODUCTION

Uric acid (UA) is produced by xanthine oxidase from xanthine and hypoxanthine, which are, in turn, produced from purine. Uric acid is more toxic to tissues than either xanthine or hypoxanthine because, at high concentrations, it may cause such diseases as hyperuricaemia, gout, and the Lesch–Nyan disease; hence, this is an important determination [1]. The modified electrodes have been reportedly developed for the single detection of ascorbic acid, dopamine, or uric acid by modifying a bare glassy carbon electrode (GCE) and a platinum–gold electrode [2–4]. Hence, a simple, rapid and suitable method is required for the regular monitoring and sensing of uric acid. In the last few decades, the detection of uric acid has been carried out using different techniques including UV-Visible, HPLC, electrochemical and enzymatic methods [5-8]. Moreover, these analytical techniques have some limitations such as being time-consuming, low-sensitive, complicated in sample preparation and economically not viable. In the last decade, nanoparticles (Au, Mn, Co, Ti, etc.), r-GO, MWCNTs [9-12], composite hybrid materials, phthalocyanine/MWCNT and CoPc–SPCEs [13-15], etc. have been used to chemically modify the electrodes to detect uric acid using cyclic voltammetry with enhanced sensitivity and selectivity. Among these methods, electrochemical measurements, particularly those using electrochemical biosensors, are most attractive for uric acid analysis because they are rapid, simple, economic and highly sensitive. In spite of their versatile electrochemical applications, very less attention was paid towards the synthesis of 2,4-dibromo-6-{[cyclohexyl(methyl)amino]methyl}aniline derivatives containing macrocyclic moiety. The present study was related to the synthesis of novel 2,4-dibromo-6-{[cyclohexyl(methyl) amino] methyl}aniline substituted cobalt phthalocyanine and exploration for the electrochemical investigations. The CoTcPc, substituted phthalocyanine enhance the solubility in organic solvents and tendency towards sensing of uric acid in PBS (pH=7) solution. The modified MWCNTs-DBCMAT-CoPcs/GCE was used for detection of micro molar solutions of uric acid using CV (cyclic voltammetry), DPV (differential pulse voltammetry) and CA (chronoamperometry) and interference studies and commercial real sample analysis using uric acid, which are in the micromolar level concentrations and most suitable for biological fluids, food, plant and animal tissue in neutral PBS electrolyte solutions.

## 2. EXPERIMENTAL

### 2.1. Precursors

2.4-dibromo-6-{[cyclohexyl(methyl)amino]methyl}aniline and tetracarboxy cobalt phthalocyanine (CoTcPc) was procured from Sigma Aldrich. N, N' dicyclohexylcarbodiimide (DCC), N, N' dimethylformamide (DMF), potassium carbonate anhydrous were procured from spectrochem Pvt, Ltd. Uric acid was purchased from Hi-Media Laboratories Pvt, Ltd. (INDIA) and used without further purifications.

### 2.2. Synthesis of 2,4-dibromo-6-{[cyclohexyl(methyl)amino]methyl}aniline-tetra substituted cobalt(II) phthalocyanine complex: (DBCMAT-CoPc )

DBCMAT-substituted on cobalt phthalocyanine is synthesized by dissolving tetracorboxy metallophthalocyanine (0.322 g, 0.0004 mol), $K_2CO_3$ (1.19 g, 0.0086 mmol) and DCC (catalyst) in dimethylformamide (DMF, 20mL) and stirred for 1hr, followed by the addition of DBCMAT (0.25 g, 0.00017 mol) to the above reaction mixture under stirring at 24 h colored precipitate appeared and reaction mixture is poured into water and repeatedly purified with ice cold water and followed by alcohol wash [16].

### 2.3. Preparation of DBCMAT-CoPc and DBCMAT-CoPcs/MWCNTs modified GC electrodes

GCE surface area was mechanically polished with 0.3 μM α-$Al_2O_3$ slurry and washed with double distilled water with deionized water, sonicated and rinsed with ethanol, and dried with room temp. Well dispersed 0.1 g of MWCNTs and 0.1 M of DBCMAT-CoPc dissolved in dry DMF solvent and sonication up to 40 min. 05 μL of suspension ink was drop casted onto the surface of GCE and dried in vacuum hot air oven and finally prepared modified MWCNTs/DBCMAT-CoPc/GC electrode and without MWCNTs is called DBCMAT-CoPc/GC electrode, after thoroughly rinsed with deionized water and (pH 7) PBS electrolyte solution. In order to avoid the oxygen interference, all electrochemical tests were carried out in $N_2$ saturated media at ~30 °C.

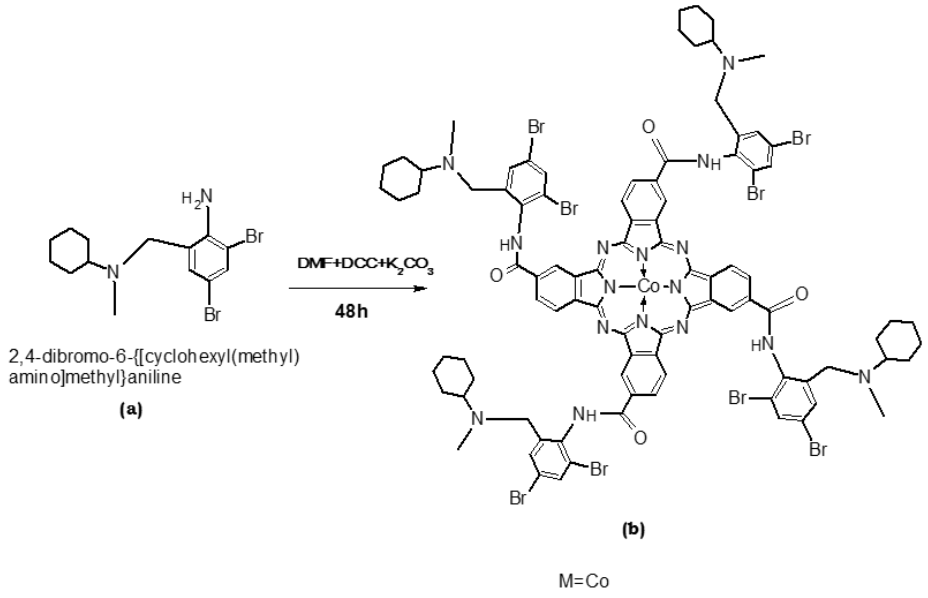


**Fig. 1.** Synthetic route of the substituted metal phthalocyanine

### 2.4. Characterization method

Ultraviolet-visible (UV-Vis) absorption spectra were recorded on Shimadzu UV-2550 spectrophotometer and infrared spectra on Perkin-Elmer spectrum 100 FT-IR spectrometer. X-ray powder diffraction patterns were recorded using a Cu Kα radiation (λ=1.5405 Å, nickel filter), on a Bruker D8 Discover equipped with a Lynx Eye detector. The data were obtained in the range of 2θ, 5–100°. The X-ray diffraction (XRD) analysis was carried out using Eva (evaluation curve fitting) software. Thermal gravimetric analysis (TGA) was recorded on a Shimadzu DTG-TG 60H with a gas flow of 120 ml/min and operated under a nitrogen atmosphere. All the electrochemical measurements were carried out on a CHI620E electrochemical workstation USA with a conventional three-electrode system (Glassy carbon electrode, Platinum wire electrode, and Ag/AgCl electrode).

## 3. RESULTS AND DISCUSSION

The synthesis of DBCMAT-CoPc complex was shown in Fig. 1. The amine group of 2,4-dibromo-6-{[cyclohexyl(methyl)amino]methyl}aniline is reacted with a carboxylic group of Cobalt phthalocyanine to yield amide bridged DBCMAT-CoPc. The elemental analysis data fairly agreed with the theoretical values indicating the synthesized complex is pure in nature. The DBCMAT-CoPc complex is blue colored in nature and readily soluble in THF and DMSO. The synthesized complex has been characterized by various spectroscopic as well as different electrochemical techniques.

### 3.1. Electronic absorption spectra

UV–Vis spectra of the DBCMAT-CoPc complex in 1 mM of N'N Dimethylsulfoxide (DMSO) solvent exhibit characteristic Q-bands and B-bands. The absorption spectra reveal the presence of Soret bands (B bands) in the range 250-360 nm and characteristic Q-band appeared in the range of 690-730 nm is attributed to the π→π* transition from HOMO to LUMO of the PCs ring, and the B band in the UV region, 300–350 nm arises from the deeper π→π* transitions [17]. Both the bands are appeared due to π→π* transitions in the CoPc molecule. The electronic absorption spectra of the complex showed characteristic absorption in the Q band region at 730 and 660 nm for DBCMAT-CoPc Fig. 2 (inset a curve), and the better-compiled results of Q and B band region to CoTcPc in Fig. 2 (inset b curve).

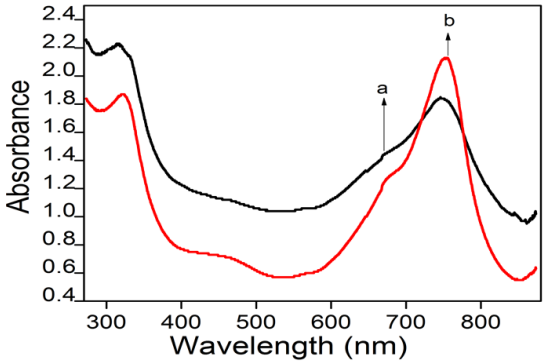


**Fig. 2.** UV-visible spectra of (a) DBCMAT-CoPc and (b) CoTcPc

### 3.2. FT-IR spectra

IR spectral data clearly indicate the formation of a compound by the appearance of new a broad peak observed in the range 3600-3200 $cm^{-1}$ for –COOH (Fig. 3 inset block curve) of CoTcPc disappears and a new peak at 3400 $cm^{-1}$ was appeared and assigned to -CONH present in the complex (Fig. 3 inset Red curve). The absorption bands at 3360- 3362 $cm^{-1}$ (-CONH), (-COOH) and (-$NH_2$) Fig. 3 inset block and red curve, 2840-2928 (Ar-CH), 1625-1628 $cm^{-1}$ for C=N, 1513-1523 $cm^{-1}$ for C=C, 1450-1452 $cm^{-1}$ for C-C, 1313, 1227, 1086, 887, 837, 741, 636 $cm^{-1}$ are attributed to the various skeletal vibration signals of CoTcPc and DBCMAT-CoPc ring and substituted ligand for Bromohexane hydrochloride as shown in Fig. 3.

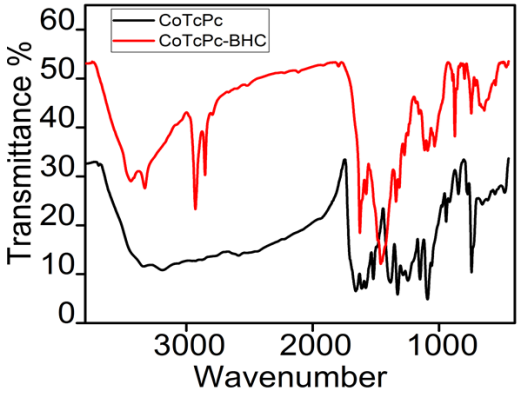


**Fig. 3.** FTIR spectra of CoTcPc (block curve), DBCMAT-CoPc (red curve)

### 3.3. Thermal properties

The thermal stability of the DBCMAT-CoPc was studied using TGA. Inset Fig. 4 b curve illustrates typical TGA thermograms of weight loss as a function of temperature from 100–600 °C. The sample (50 mg) was heated from room temperature to 600 °C at the rate of 5 °C/min in nitrogen. The TGA curve (above) is labeled in terms of the identity of the complex. The temperature range 100-400 °C (57% weight loss of substituted ligand), 400-550 °C (22%

weight loss of Pc ring) Pc complex and 550-600 °C (21 % weight loss of CoO). The degradation temperature was found to vary as a function of temperature. Inset Fig. 4 b curve shows that the thermal stability of the DBCMAT-CoPc complex was higher than that of pure CoTcPc where the degradation temperature is significantly shifted to higher values (Inset Fig. 4 b curve) [18,19]. The synthesized DBCMAT-CoPc is a high thermally stable as compare to bare CoTcPc as shown in Fig. 4.

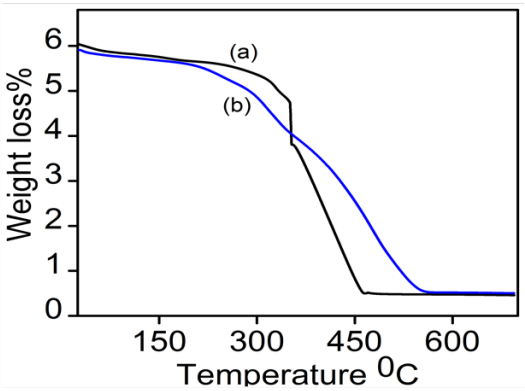


**Fig. 4.** TGA of (a) CoTcPc (b) DBCMAT-CoPc

### 3.4. X-ray Diffraction Analysis

X-ray powder diffraction (XRD) was employed to elucidate the crystal nature and size of the substituted CoPc. The patterns are qualitative and are similar to that of DBCMAT-CoPc; however, the pattern was more dispersive in intensity than the corresponding metal phthalocyanine. The XRD pattern was used to explain qualitatively the degree of crystallinity [20]. The XRD pattern indicates that the obtained DBCMAT-CoPc is amorphous in nature. The 15, 17, 23, 26, 45, 47, 53, 58, 65, 71 peaks that were observed at room temperature disappeared and four other lines emerged (Fig. 5). This peak corresponds to long aliphatic chains that are located randomly within the columnar mesosphere with an average spacing of 4.6 Å. A less broad peak was found around 3.4 Å, which was the stacking distance of phthalocyanine core within the columns. These results are similar to the data of the DBCMAT-CoPc obtained [21]. The observed patterns are very much similar to parent phthalocyanines except the broadening of the peaks. The broadening may be due to the presence of substituent and which seems to play an important role in the stacking of the substituted phthalocyanine derivative.

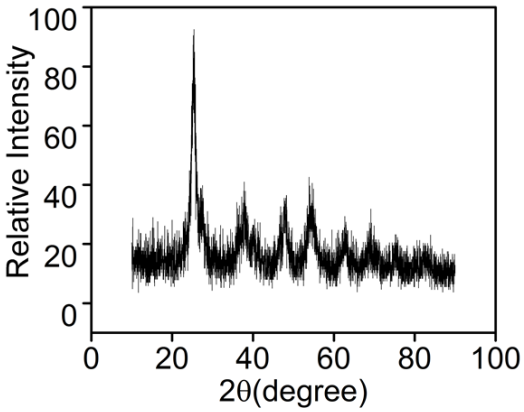


**Fig. 5.** X-ray diffractograms of DBCMAT-CoPc

*3.4.1. Electrochemical Characterization of Modified Electrodes*

Characterization of the modified electrodes was carried out in pH 7 PBS and modified DBCMAT-CoPc/MWCNT/GCE using cyclic voltammetry to determine their properties in synthesized complex metal (Co) oxidation behavior. Fig. 6 (i) illustrate comparative current response results obtained with the bare GCE, and modified with MWCNTs electrodes, and an enhanced current response for the GCE modified with DBCMAT-CoPc/MWCNTs/GCE (inset Fig. 6 curve(ii)) and the bare GCE was no current response inset Fig. 6 curve (i). When GCE was modified with DBCMAT-CoPc/GCE, the high current response was observed as compared to bare GCE. The cyclic voltammetric curve showed that the phthalocyanine complexes exhibited one oxidation peak indicating that the synthesized complex is electroactive in nature.

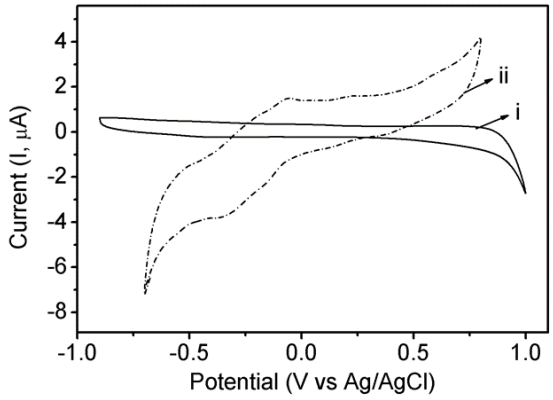


**Fig. 6.** CV profile for the i) bare and ii) DBCMAT-CoPc/MWCNT/GCE phthalocyanine complex in PBS pH 7 at 50 mV $s^{-1}$ under detreated condition using $N_2$

*3.4.2. Charge Transfer Behaviour of the Modified electrodes*

The charge transfer behavior of the substituted cobalt phthalocyanine electrode was studied using 10 μM $K_4[Fe(CN)_6]$ which acts as a redox probe. Fig. 7 shows the cyclic voltammograms

for the $[Fe(CN)_6]_3/[Fe(CN)_6]_4$-redox couple on the bare glassy carbon electrode and modified electrodes. The bare GCE shows the typical ferri/ferrocyanide cyclic voltammetric response whereas the DBCMAT-CoPcs/GCE showed slightly blocking or diffusive behavior (inset Fig. 7 curve ii). It is known that less conductive macrocycles are prone to inhibiting current flow and immobility of ions. But the composite electrode (DBCMAT-CoPc/MWCNT/GCE) showed faster and efficient electron transfer rate with lesser ΔE separation between the cathodic and anodic peak potentials as well as an increase in the peak currents. This may be due to the presence of high surface area MWCNTs which behaves as good conductor and mediates the electron transfer between electrode and electrolyte (inset Fig. 7 curve iii). The composite acts as an electronic conductor and it provide the extra surface to absorb the charges and reaction to happen. The modified electrode was detecting good electronic conductor of this synthesized macrocyclic compound responses for modified glassy carbon electrode.

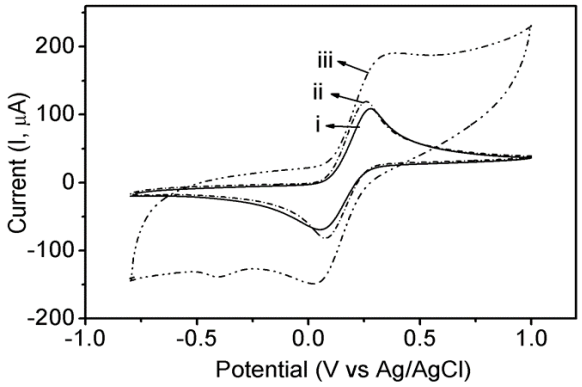


**Fig. 7.** Charge transfer behavior of the **i)** bare GCE and **ii)** GCE/DBCMAT-CoPc and **iii)** GCE/DBCMAT-CoPc-MWCNT electrodes in phosphate buffer with 0.1 mM $K_4[Fe(CN)_6]$ at 50 mV $s^{-1}$

*3.4.3. Electroanalytical oxidation-reduction reactions*

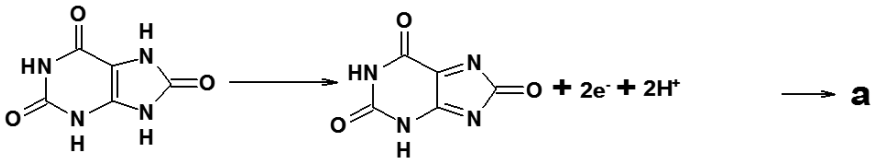


**Scheme 1.** Analytes oxidation-reduction reactions of uric acid oxidation

*3.4.4. Effect for Concentrations Uric acid Detections*

The electrocatalytic activities of DBCMATCoPc/MWCNTs modified GCE towards various concentrations of UA are depicted by cyclic voltammograms at a scan rate of 50 $mVs^{-1}$. Fig. 8A displays the concentration dependence of uric acid at DBCMAT-

CoPc/MWCNTs/GC electrode. As expected, no redox peaks can be observed in the pH 7 blank solutions. After addition of different concentrations of uric acid from 0.1 to 1.8 µM, a well-defined and redox peaks located at 370 mV *vs*. SCE appeared with the linear relationship between the peak currents and the different concentrations. The study suggests that the proposed sensor proved to be good electrocatalytic activity towards uric acid oxidation; the positive peak current of uric acid at DBCMAT-CoPc/MWCNTs/GCE has a meager increase than that of without UA (Fig. 8 black line curve) and exhibit a large background current with a weak redox peak for UA and cathodic ($E_{pc}$) peak potentials at 370 mV (Fig. 8A). A well-defined oxidation peaks was also observed for DBCMAT-CoPc/MWCNTs/GCE, indicating that the oxidation reaction of UA occurred at the electrode surface. These phenomena's were clear pieces of evidence of the catalytic effect of the chemically modified electrode toward UA oxidation [22,25]. The linear response of DBCMAT-CoPc/MWCNTs/GCE towards the different concentrations of UA vs cathodic peak current ($I_{pc}$); Y=17.887 (UA)+8.656 with correlation coefficient of $R^2$=0.9978 (inset Fig. 8b).

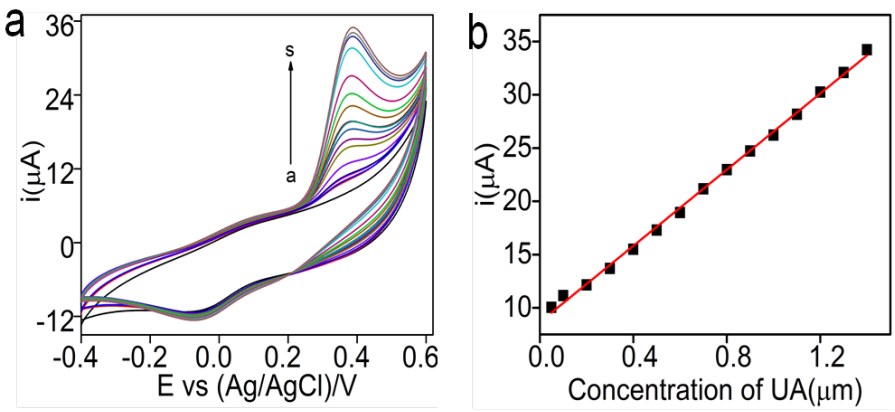


**Fig. 8.** CVs plot of; (a) modified GCE of Different concentrations (0.1-1.8 µM) of uric acid, at scan rates 50 mV/s and (b) Linear plot of peak current *vs* concentration of uric acid

### *3.4.5. Effect of scan rate*

Fig. 9a shows the different scan rates (10-200 mV $s^{-1}$) of 0.5 µM uric acid with well-defined peak potential and intermediate peaks at the same positive current and a linear relationship was established between the positive peak current and the square root of scan rate. The linear equations were expressed as follows: uric acid: $I_{pa}$ (µA)=131.859 $\upsilon^{1/2}$ ($mVs^{-1}$)+1.121, $R^2$=0.9999 (inset Fig. 9b); the above results indicate that the oxidation of uric acid on DBCMAT-CoPc/MWCNTs/GCE was a diffusion controlled process, the detection limit of 0.033 µmol/L, linear concentration range from 0.1 to 1.8 µmol/L and sensitivity of 131.859 $\mu A \mu M^{-1} cm^{-2}$ Table 1 [26].

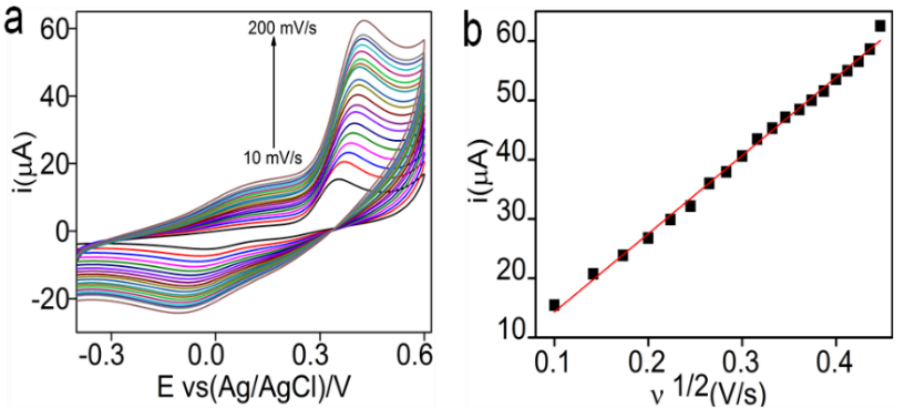


**Fig. 9.** Experimental CVs peaks at: (a) Different scan rates of uric acid (10-200 $mVs^{-1}$) and (b) Linear plot of peak current v/s different scan rates/$mVs^{-1}$

*3.4.6. Differential pulse voltammetry studies of uric acid*

Fig. 10 shows the DPV recordings at various concentrations of uric acid at the DBCMAT-CoPc /MWCNTs/GCE at the scan rate of 50 mV $s^{-1}$. The concentration range of UA was 0.2-1.8 µM, and the concentration range of DBCMAT-CoPc/MWCNTs/GCE was 0.2~2.8 µM and detection for positive potential 370 mV. The results showed that the oxidation peak currents increased with the increase in the concentrations of uric acid Fig. 10. The oxidation current of UA was proportional to the concentration of uric acid, following the linear regression equation is: $I_p$ (µA)=22.634×[UA] (µM)+6.095 inset Fig. 10. The plots showed good linearity, with a correlation coefficient of 0.99417 and the detection limit of 0.066 µM (where s/n=3), linear concentrations range from 0.2-2.8 µmol/L and sensitivity for 22.633 $\mu A \mu M^{-1} cm^{-2}$. The analytical good performance of modified GCE and compare to a literature survey as shown in Table 1.

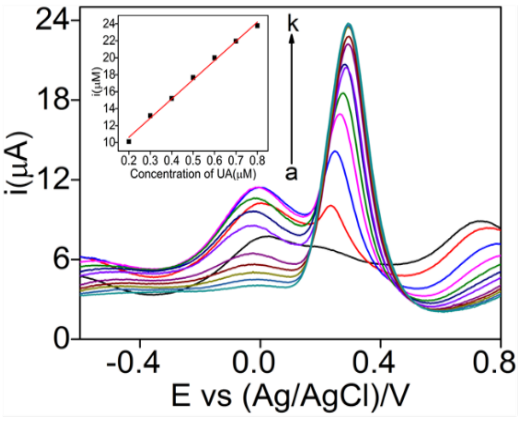


**Fig. 10.** Experimental DPV peaks at modified electrode and Different concentrations of uric acid and inset linear plot of positive peak current vs different concentrations of uric acid/µM

**Table 1.** Performance of the proposed sensors with some modified electrode used for the determination of uric acid

| **Electrodes** | **Methods** | **Linear range (µmol/L)** | **Sensitivity ($\mu A \mu M^{-1}$)** | **LOD (µmol/L)** | **Ref.** |
|---|---|---|---|---|---|
| UOx/BSA/BLGMWCNT sPtNPs/GCE | CA | 20 - 500 | 31.131 | 0.8 | [27] |
| Uricase/HRP-cds | CV | 125-1000 | - | 125 | [28] |
| GCE-CoPc/MWCNT | SW | 200-1000 | - | 260 | [29] |
| RGO/GCE | CA | 2–600 | - | 1.0 | [30] |
| DBCMAT-CoPc /MWCNT/GCE | CV | 0.1-1.8 | 131.85 | 0.03 | This work |
| | DP | 0.2-2.8 | 22.634 | 0.066 | |
| | CA | 0.05-0.9 | 2.509 | 0.016 | |

*3.4.7. Amperometry responses of uric acid*

The modified GCE based sensor was probed further using amperometry Fig. 11a. Initially, only PBS pH 7 was present in the cell. Stirring was initiated; the electrode was poised at a selected working potential +0.500 V for UA, the modified DBCMAT-CoPc/MWCNT/GCE was detection of uric acid with high enhancing positive peak current (Fig. 11a) to the successive addition of uric acid into the PBS pH 7.

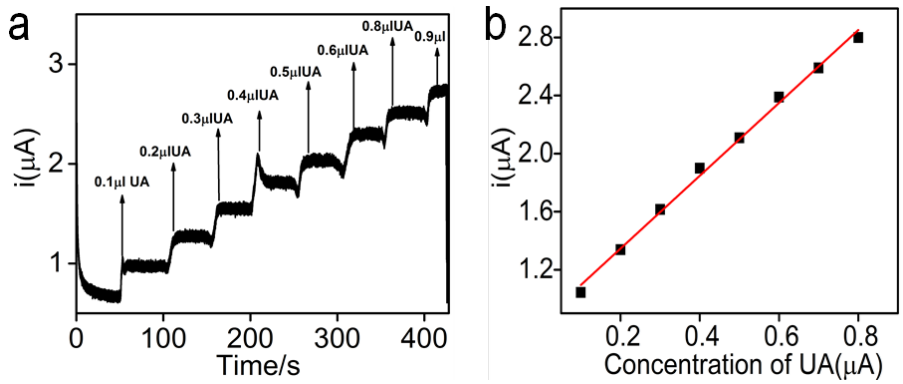


**Fig. 11.** An experimental Amperometry uric acid peaks at: (a) Different concentrations of uric acid and (b) Linear plot of Ip v/s different concentrations of uric acid. Applied potential +0.5V

The DBCMAT-CoPc/MWCNTs/GCE was found to exhibit a linear response to additions of uric acid up to different concentration [27]. After which the noise generated by stirring precluded the accurate measurement of the current. Inset Fig. 11a curve describes the response of uric acid with the addition of different concentrations for 0.05 to 0.9 µM. The linear equation of peak current ($I_p$) *vs.* different concentrations of uric acid (Fig. 11b) was described as Ip

(μA)=2.509(UA)+0.8443, with correlation coefficient ($R^2$) of 0.9955. The linear concentration range, sensitivity, detection limit were 0.05 to 0.9 μM, 0.016 $\mu A \mu M^{-1} cm^{-2}$, at a signal-to-noise ratio (S/N) of 3 (Table 1). Magnified portion of the amperometry response curve for addition of UA solution with very low concentration was shown in Fig. 11a.

### *3.4.8. Amperometry interference responses of uric acid by DBCMAT-CoPc/MWCNTs/GCE*

The Interference amperometry responses of tetra DBCMAT-CoPc/MWCNTs/GCE in PBS (pH=7) electrolyte solution: Interfering species for (0.5 μM for Glucose, L-Cysteine, Tyrosine, $H_2O_2$ and Glycine) and 0.2 μM of uric acid at the potential of +0.500 V. Fig. 12, exhibits the five interfering species generated a completely negligible current response as compared to the high current responses to 0.2 μM UA, indicating high selectivity for the UA [27]. The high selectivity could be attributed to the following two reasons: On one hand, the relative low potential for detection could greatly minimize the responses of common electroactive interference. On the other hand, the presence of Nafion in the DBCMAT-CoPc/MWCNTs/GCE also facilitated to diminish the interferences since the good selectivity interfering species (e.g. Glucose, Ascorbic acid, $H_2O_2$, and Glycine) from permeating into the electrode surface as shown in Fig. 12.

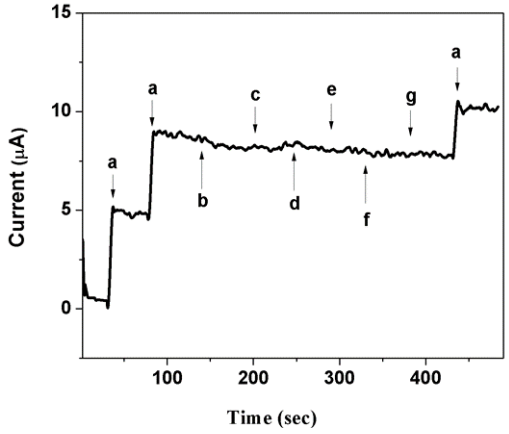


**Fig. 12.** Amperometric i-t response for the addition of a) 0.05 uric acid and 0.1 μM of (b) glucose, (c) ascorbic acid, (d) $H_2O_2$, (e) Glycine, (f) Tyrosine, and (g) L-Cysteine, in pH 7 PBS *at* GCE/ DBCMAT-CoPc (applied potential of 0.5 V)

### *3.4.9. Stability Studies*

The stability of the fabricated sensors towards uric acid determination was investigated at 10 repeated CV scans in pH 7 PBS containing 0.5 μM of uric acid at a scan rate of 50 mV $s^{-1}$ figure not shown the stability was investigated using DBCMAT-CoPc/MWCNTs/GCE modified electrode. From the repeated scans, it was found that the peak current of the first cycle

was more than the peak current of the second cycle and after the third cycle; there was no significant drop in the current response. This behavior was observed with all the four modified electrodes. Therefore the percentage current drop obtained was 5.65%, DBCMAT-CoPc-MWCNTs/GCE modified electrode respectively. Thus, the peak currents (1st to 10th cycles) remained almost stable, indicating good electrodes stability during repeated cycles. These results suggest that there is some level of adsorption of UA at electrodes surface. The adsorptive nature of electrodes might be due to the porous-structured film of the CNTs on the electrodes [26].

### *3.4.10. Reproducibility and repeatability Studies*

The modified electrode of DBCMAT-CoPc-MWCNTs/GCE was constructed in four sets to determine the reproducibility and in turn, precision of the analysis. The detection of uric acid (0.5 μM) was performed on the modified DBCMAT-CoPc-MWCNTs/GC electrode by amperometry method. The RSD was calculated and found to be 2.1% for DBCMAT-CoPc-MWCNTs/GCE modified electrodes. The sensor repeatability was performed for the detection of uric acid (0.5 μM), by taking five repeated amperometry measurements using the same DBCMAT-CoPc-MWCNTs/GCE electrodes. The fabricated sensors endorse satisfactory reproducibility (2.1%) and repeatability (RSD-1.9%).

### *3.4.11. Real sample analysis*

**Table 2.** Recovery analysis of uric acid, and dopamine in urine samples using DBCMAT-CoPc /MWCNT/GCE

| **Samples** | **Biomolecules detected** | **Found (μmol $L^{-1}$)** | **Spiked (μmol $L^{-1}$)** | **Recovered in total (μmol $L^{-1}$)** | **Recovery (%)** |
|---|---|---|---|---|---|
| Urine 1 | DA | - | 10 | 9.9 (±0.5) | 99 |
| | UA | 16.5 | 5 | 21.8 (±0.8) | 106.0 |
| Urine 2 | DA | - | 15 | 15.1(±1.1) | 100.6 |
| | UA | 18.5 | 10 | 28.3 (±1.3) | 98 |
| Urine 3 | DA | - | 20 | 20.3 (±0.4) | 101.5 |
| | UA | 24.7 | 15 | 40 (±0.8) | 100.7 |

The real sample analysis was carried out using urine sample for the detection of uric acid and dopamine. Since, the urine sample showed measurable amount of uric acid only and no dopamine. Hence, the spiking method was used for the analysis i.e., standard addition method by adding known concentration of UA and DA into the urine sample. 1 mL urine sample was added to 10 mL PBS pH 7. electrolyte. The appropriate recovery of the ternary mixture is

summarized in the Table 2. The DBCMAT-CoPc/MWCNT/GCE electrode ensured the practical feasibility in the detection of UA and DA biomolecules in real samples Table 2.

## 4. CONCLUSION

The novel synthesized title compound was confirmed by various physicochemical characterization techniques of FT-IR, UV, TGA, XRD spectra. In summary, we present a rarity sensor material that was based on uric acid oxidation for the covalent modification of GCE and it seems to offer a fast, economically reliable and simple for quantifying uric acid ac. The findings of this study indicate that the DBCMAT-CoPc/MWCNTs/GCE exhibit electrochemical sensing oxidation of uric acid. From our results we claim the following advertence: (a) UA irreversible is increased at DBCMAT-CoPc/MWCNTs/GCE that have more considerable advantages in electroanalytical application using composite MWCNTs, (b) neutral PBS electrolyte showed good performances in uric acid analyte with significant current responses, (c) sensitivity, low detection limit for CVs, DPV and amperometry techniques. The well-defined positive potential and good responses of amperometry interference sensing studies with negligible current responses for Glucose, Ascorbic acid, Glycine, Tyrosine, $H_2O_2$, and L-Cysteine. This work proves that it can be successfully used for determination of commercial uric acid in human urine samples for satisfactory results, and the modified GCE was a good and attractive candidate for practical applications.

**Acknowledgement**

One of the author Malathesh Pari Thanks to VGST (GRD No 229), Government of Karnataka for the financial support

## REFERENCE

[1] V. V. S. E. Dutt, and H. A. Mottola, Anal. Chem. 46 (1974) 1777.
[2] A. Cizewski, and G. Milzarek, Anal. Chem. 71 (1999) 1055.
[3] Y. Li, and X. Lin, Sens. Actuators b 115 (2006) 134.
[4] G. Jin, Y. Zhang, and W. Cheng, Sens. Act. B 107 (2005) 528.
[5] C. W. Liao, J. C. Chou, T. P. Sun, S. K. Hsiung, and J. H. Hsieh. IEEE Trans Biomed Eng. 53 (2006) 1401.
[6] H. C. Hong, and H. J. Huang, Anal. Chem. Acta (2003) 41.
[7] R. Kock, B. Delvoux, and H. Greiling. Eur. J. Clin. Chem. Clin. Biochem. 31 (1993) 303.
[8] A. A. Ensafi, M. Taei, T. Khayamian, and A. Arabzadeh, Sens. Act. B 147 (2010) 213.
[9] K. S. Lokesh, A. Shambhulinga, N. Manjunatha, M. Imadadulla, and M. Hojamberdiev, Dyes and Pigments 120 (2015) 155.

[10] K. S. Lokesh, V. Narayana, and S. Sampatha. Microchim. Acta 167 (2009) 97.
[11] T. N. Rajesh, J. Keshavayya, M. N. K. Harish, A. S. R. Ali, and C. K. T. Kumar. Res. J. Chem. Sci. 11 (2013) 36.
[12] R. N. Goyal, V. K. Gupta, N. Bachheti, and R. A. Sharma, Electroanalysis 20 (2008) 757.
[13] J. de Ftima Giarola, and A. Cesar Pereira, Electroanal. 28 (2016) 1348.
[14] P. Kanyong, R. M. Pemberton, S. K. Jackson, and J. P. Hart, Anal. Biochem. 428 (2012) 39.
[15] J. Arora, S. Nandwani, M. Bhambi, and C. S. Pundir, Anal. Chem. Acta 647 (2009) 195.
[16] M. Pari, Mounesh, B. S. Jilani, and K. R. Venugopala Reddy, Anal. Bioanal. Electrochem. 11 (2019) 460.
[17] A. Yavuz, B. Bezgin, L. Aras, and A. M. Onal. J. Electroanal. Chem. 639 (2010) 116.
[18] J. P. Fan, X. M. Zhang, and M. Ying. J. Chem. 63 (2010) 145.
[19] Mounesh, Bhvimane sanna jilani, Malathesh. Pari, K. R. Venugopala Reddy, and K. S. Lokesh. Microchem. J. 147 (2019) 755.
[20] K. Sawada, W. Duan, K. Sekitani, and K. Satoh, J. Mol. Liq. 119 (2005) 171.
[21] J. Sleven, C. Görller-Walrand, and K. Binnemans, Mater. Sci. Eng. C 18 (2001) 229.
[22] C. C. Vishwanatha, B. E. Kumara Swamy, and K. Vasantakumar Pai, J. Anal. Bioanal. Tech. 6 (2015) 237.
[23] S. Shahrokhian, and H. R. Zare-Mehrjardi, Electroanal. 19 (2007) 2234.
[24] U. Yogeswaran, S. Thiagarajan, and S. M. Chen, Anal. Biochem. 365 (2007) 122.
[25] S. Shahrokhian, and H. R. Zare Mehrjardi. Electroanal. 19 (2007) 2234.
[26] J. de Fatima Giarola, and A. Cesar Pereira, Electroanal. 28 (2016) 1348.
[27] B. Han, M. Liu, J. Liu, T. Cui, and Quian Gchen, Materials 12 (2019) 214.
[28] E. Azmine, N. Ramli, J. Abdullah, M. A. Abdul Hamid, H. Sidek, S. Abd Rahman, N. Ariffin, and N. A. Yusof, Biosens. Bioelectron. 67 (2015) 129.
[29] M. Nemakal, S. Aralekallu, I. Mohammed, M. Pari, K. R. Venugopala Reddy, and L. Koodlur Sannegowda, Electrochim. Acta 318 (2019) 342.
[30] H. Wang, F. Ren, A. Wang, B. Yang, D. Bin, and Yukoudu, RSC Adv. 4 (2014) 26895.